Translational Oncology
www.transonc.com

Volume 12 Number 1 January 2019 pp. 122–133 122

Phenotypic and Expressional Heterogeneity in the Invasive Glioma Cells[1,2]

Artem Fayzullin[*], Cecilie J. Sandberg[*], Matthew Spreadbury[*], Birthe Mikkelsen Saberniak[*], Zanina Grieg[*], Erlend Skaga[*], Iver A. Langmoen[*,†] and Einar O. Vik-Mo[*,†]

[*]Vilhelm Magnus Laboratory for Neurosurgical Research, Institute for Surgical Research, Oslo University Hospital, Oslo, Norway; [†]Department of Neurosurgery, Oslo University Hospital, Oslo, Norway

Abstract

BACKGROUND: Tumor cell invasion is a hallmark of glioblastoma (GBM) and a major contributing factor for treatment failure, tumor recurrence, and the poor prognosis of GBM. Despite this, our understanding of the molecular machinery that drives invasion is limited. *METHODS:* Time-lapse imaging of patient-derived GBM cell invasion in a 3D collagen gel matrix, analysis of both the cellular invasive phenotype and single cell invasion pattern with microarray expression profiling. *RESULTS:* GBM invasion was maintained in a simplified 3D-milieue. Invasion was promoted by the presence of the tumorsphere graft. In the absence of this, the directed migration of cells subsided. The strength of the pro-invasive repulsive signaling was specific for a given patient-derived culture. In the highly invasive GBM cultures, the majority of cells had a neural progenitor-like phenotype, while the less invasive cultures had a higher diversity in cellular phenotypes. Microarray expression analysis of the non-invasive cells from the tumor core displayed a higher GFAP expression and a signature of genes containing VEGFA, hypoxia and chemo-repulsive signals. Cells of the invasive front expressed higher levels of CTGF, TNFRSF12A and genes involved in cell survival, migration and cell cycle pathways. A mesenchymal gene signature was associated with increased invasion. *CONCLUSION:* The GBM tumorsphere core promoted invasion, and the invasive front was dominated by a phenotypically defined cell population expressing genes regulating traits found in aggressive cancers. The detected cellular heterogeneity and transcriptional differences between the highly invasive and core cells identifies potential targets for manipulation of GBM invasion.

Translational Oncology (2019) 12, 122–133

Introduction

Glioblastoma (GBM) is the most frequent and malignant brain cancer. Standard treatment only extends the life of patients with months, and the median survival in unselected patient populations is less than a year [1]. The tumors' ability to invade into the surrounding brain parenchyma is a major challenge as it makes complete resection unachievable. The invasive cells left in the brain after tumor resection are resistant to chemo- and radiotherapy and are thus responsible for the inevitable tumor recurrence [2,3].

GBM cells have the ability to move through the highly packed neuropil, but rarely enter into the circulation [4]. Thus, the invasion of glioma cells is different from the metastatic spread of other cancer cells and is likely dependent on a unique set of molecular pathways [5]. Moreover, GBMs display high levels of inter- and intratumoral

Address all correspondence to: Artem Fayzullin, Vilhelm Magnus Laboratory for Neurosurgical Research, Institute for Surgical Research, Oslo University Hospital, P.O. Box 4950 Nydalen, Oslo, Norway. E-mail: artem.fayzullin@rr-research.no

[1] Funding: This work was supported by Norwegian Cancer Society (Kreftforeningen, grant *2326811*), The Research Council of Norway through Cancer Stem Cells Center for Research Based Innovation (SFI-CAST) and the Department of Neurosurgery, Oslo University Hospital.

[2] Conflict of interest: The authors declare that they have no conflict of interest.

Received 16 June 2018; Revised 21 September 2018; Accepted 24 September 2018

1936-5233/19
https://doi.org/10.1016/j.tranon.2018.09.014

heterogeneity, where only a subset of the tumor cells is invasive [5]. To understand the glioma-specific properties of invasion, models must recapitulate the heterogeneous cellular phenotype seen in patients while being simple enough to allow for interpretation.

To experimentally decipher the ability of glioma tumor cells to migrate and invade into the brain, it is essential that the model system retains this key characteristic of GBM. The traditional long term serum cultivated GBM cell lines express markers suggesting neural lineage, but display molecular characteristics more common to other cell lines than the tumor of origin [6]. Upon transplantation to the brain these cells establish rapidly growing tumors, but with sharply delineated borders to the brain parenchyma – more resembling brain metastases than glial tumors [7,8]. In contrast, the use of patient-derived GBM tissue allows for isolation of cells with invasive properties. These cells can be propagated as tumorspheres under serum-free, growth factor-enriched media and establish phenocopies of the parent tumor in serial xenotransplantation [7,9,10]. Importantly, these induced tumors are highly invasive, harboring cells that migrate widely throughout the brain [9,11–13].

The specific biological behavior of invasive GBM cells suggests the activation of certain genetic programs that distinguish them from cells in the tumor core [14]. While global expression profiles of glial tumors have been studied extensively, less is known about specific gene expression in the invasive cells [15,16]. The experimental studies exploring transcriptional differences associated with invasion in brain slices [17] or in vivo xenograft models [18] do not use real-time observations that allows for analysis of movement patterns. Thus, an approach that allows transcriptome analysis of invading GBM cells with identified differences in invasive capacity by real time observation has been called for [19].

We have previously described the phenotype and invasive characteristics of invading glioma cells in organotypic brain slices. Here we present studies on real-time quantification of human GBM cell invasion with comparative analysis of transcriptional profiles in non-invasive and invasive cells. Using a simple collagen 3D matrix system, we demonstrate how this system maintains the invasive characteristics found in more complex systems and how it allows for the detection of intra- and intertumoral heterogeneity to understand mechanisms of glial cell invasion.

Materials and Methods

Cell Culture

GBM biopsies were obtained from informed and consenting patients after approval by the Norwegian National Committee for Medical Research Ethics (07321b). The biopsies were dissociated into single cells and cultured in a serum-free medium supplemented with bFGF and EGF as previously described [20]. Seven primary cell cultures were established from brain tumor biopsies, all from IDH wild-type, treatment-naïve GBMs, of which one was classified as a giant cell GBM. Two of these cultures have previously been described (T0965, T1008) [12,21,22]. The tumorigenicity of all cultures was confirmed upon xenografting to SCID mice. The tumorspheres in the cultures displayed heterogeneous morphology and growth pattern characteristics, with population doubling times ranging from 2 to 8 days.

Grafting of GBM Cultures for Time-Lapse Microscopy

The plating of tumorspheres on fibronectin-coated plates and into rodent brain slices was performed as previously described [12,23]. For grafting tumorspheres into collagen gel rat collagen I protein (0.5 mg/ml) (Gibco) was prepared according to the manufacturer's recommendation and distributed as 30 µl drops in 24 well plates, before single tumor spheres of 150 to 250 µm were grafted into the gel by a 2 µl pipette. For cell-suspension grafting 2 µl containing approximately 500 cells was used. In experiments where tumorspheres were co-grafted with cell suspension verification of cell origin, whether single cell in suspension or sphere, was done by tracking cells by time-laps imaging starting immediately after grafting. After 30 to 45 min of gelation at 37 °C in cell incubator, grafts were supplemented with 200 µl of tumor sphere medium supplemented with 1% foetal bovine serum (FBS).The time-lapse imaging was performed on Olympus IX81 inverted fluorescence microscope with a temperature and environmental gas supply control. The time-lapse experiments lasted from one to 5 days with imaging every 20 min. Images were acquired using Olympus Soft Imaging Xcellence software.

Quantification of Invasive Parameters

For quantification of directionality and migratory velocity, post-processing of the images was performed using the ImageJ package Fiji with a manual cell tracking plug-in. The manual tracking was performed by two independent researches. Directionality is the ratio between the length of a straight line between the start and endpoint of migration to the total accumulated distance and was calculated by Ibidi Chemotaxis and Migration Tool. Total invasive increment is the sum of all distances that invasive cells have moved from the tumorsphere. It was identified by nuclear-stained grafts analyzed by ImageJ software with the "Find Maxima" option. The obtained total number of invasive cells and their X/Y coordinates were transferred to Microsoft Excel.

Immunochemistry

Gels were washed with phosphate buffered saline (PBS) and fixed with 4% paraformaldehyde for 15 min. Then, the samples were processed as described previously [6] with primary antibodies against nestin (mouse, 1:500, Abcam), β-III-tubulin (rabbit, 1:1000, Sigma) and GFAP (rabbit, 1:1000, Dako), MAP2 (mouse, 1:500, Millipore), Ki-67 (rabbit, 1:500, Santa Cruz), CTGF (goat, 1:100, Santa Cruz), synemin (rabbit, 1:200, Sigma Aldrich), TNFRSF12A (rabbit, 1:100, Sigma Aldrich), annexin A1 (goat, 1:200, R&D Systems) and anti-mouse AlexaFluor 488 (donkey, 1:500, Invitrogen) and anti-rabbit AlexaFluor 647 (donkey, 1;500, Invitrogen) secondary antibodies.

For immunostaining of membrane surface receptors the GBM spheres were incubated prior to grafting in 4 °C for 20 min with fluorescent-conjugated antibodies (1:20 dilution in 2% FBS in PBS) and washed twice. Antibodies used were anti- CD166 (PE, BD Pharmingen), CXCR4 (PE, Miltenyi Biotec), CD29 (FITC, Chemicon), CD133 (PE, Miltenyi Biotec), CD44 (APC, eBioscience), CD9 (FITC, eBioscience).

Grafting of Tumorspheres into Collagen Gel for the Isolation of the Invasive Cells

After 2 days in incubator, gels were treated with collagenase (10 mg/ml) (Sigma) in PBS, and visually confirmed for the separation of cores and invasive cells, before the mixture was passed through a 40 µm cell filter to separate the invasive cells from graft cores. The cells were spun down twice before the precipitates were further processed for western blot, qPCR or microarray.

Western Blot

Western blot and quantification of protein expression was performed as previously described [21].

Quantitative Real-Time PCR (qPCR) and Microarray Analysis

Total RNA was extracted using the RNeasy Micro Kit (Qiagen). Quality control and cDNA synthesis was performed as previously described [24]. For qPCR we used the TaqMan Fast Advanced Master Mix and the following predesigned TaqMan oligonucleotide primers and probes (Applied Biosystems): Hs00157674_m1 (GFAP), Hs9999999903_m1 (ACTB), Hs009985_g1 (CYR61), Hs03676575_s1 (ID1), Hs00375306_m1 (PMEPA1), Hs00167549_m1 (ANXA1), Hs00954037_g1 (ID3), Hs00159652_m1 (NPTX1), Hs00745167_sH (MT1X), Hs00270931_s1 (CEBPD), Hs01072228_m1 (CHI3L1), Hs00293956_m1 (DDIT4L) and HS00959047_g1 (TNFRSF12A). The thermal cycling conditions were 20 seconds at 95 °C, followed by 40 cycles of 1 second at 95 °C and 20 seconds at 60 °C. The relative gene expression levels were calculated using the standard curve method. For microarray analysis, the RNA samples were run on a HumanHT-12 chip (Illumina). Analysis and statistics were performed using J-Express (Molmine). Differential gene analysis was carried out using RankProd [25].

Statistics

GraphPad Prism 6.0 was used for statistics analysis and graphical presentation. Statistical analysis of difference between groups was undertaken using unpaired t-test. The results were considered significant if $P < .05$. Experiments were done in independent triplicates, unless otherwise stated. Error bars in graphical presentations represent standard error of the mean.

Results

GBM Cellular Invasion is Maintained in a Simplified 3D-Milieue by the Presence of the Core

We have previously demonstrated the phenotype and invasive dynamics of migrating GBM cells in organotypic rat brain-slice cultures [12]. Cells plated on fibronectin are widely used for evaluating migration in the "scratch-assay", while 3D protein matrixes are suggested as better models to study glioma cell invasion [26]. To allow higher resolution imaging on a single cell level and minimize the effects of a heterogeneous extracellular environment, we compared the phenotype and motility pattern of glioma cells in these conditions to cells grafted into brain-slice cultures (Figure 1, Mov. 1). Cells plated on a fibronectin-coated plastic surface displayed sheet-like or fusiform morphology without exhibiting a constant leading process. Their migration was non-directional and associated with random formation of lamellipodia. After attachment of a tumorsphere to the surface, cells migrated out into a confluent monolayer. In contrast, tumorspheres grafted into a 3D collagen matrix developed a halo of invading cells. The majority of invading cells in the collagen matrix adopted a neural progenitor-like phenotype with a round small cell body and a long leading process. This is the same Type I cells that we found to dominate the invasion in organotypic brain-slice cultures [6]. These cells have elongated cell bodies with a diameter of 5 to 25 μm, and a distinct leading process with a length more than 3 to 5 times longer than the cell body. Cellular heterogeneity was present among the invasive cells, and all the cell types described in brain-slice cultures (Type II, giant cells and cells with random morphology) were also found in collagen matrix (data not shown).

We have previously described how signaling cues from the tumorsphere induced and oriented the migratory spread of invasive tumor cells in organotypic brain slice cultures [12]. We verified this in tumorspheres transplanted to collagen matrix using three different experimental setups (Figure 1 and Mov. 2 and 3). First, we dissociated GBM tumorspheres to single cell suspension before grafting into collagen matrix. When no tumorsphere was present, the cells migrated in a non-directional, random manner. Secondly, we performed grafting of single cell suspension to collagen matrix, followed by co-grafting of tumorspheres from the same tumor. After the tumorsphere was co-grafted, a fraction of the cells located close to the sphere acquired directional, radial movement away from the sphere. However, not all cells reacted to the co-grafting. A fraction of the cells, even close to the spheres, did not respond to the presence of the sphere by initiation of directed migration. These cells continued to move randomly, skipping past the passing stream of invading cells. Thirdly, we grafted tumorspheres into the collagen matrices and then removed the tumor cores by microsurgical resection after 24 hours. The resection of the tumor core interrupted the directional invasive migration of cells, resulting in a reduction of the invasive increment sum and directionality. In tumor T0965 the invasive increment was 281.3 ± 10.7 μm vs. 33.3 ± 2.3 μm ($P < .01$) and directionality 0.86 ± 0.01 vs. 0.19 ± 0.01 ($P < .01$), before and after core resection, respectively. In tumor T1402 the invasive increment was 431.7 ± 22.9 μm vs. 101.7 ± 33.6 μm ($P < .01$) and the directionality 0.78 ± 0.02 vs. 0.24 ± 0.03 ($P < .01$). In the control grafts, the majority of cells continued the invasive migration away from the core. Thus, without a tumor core, cells migrated randomly, however by introducing a tumorsphere targeted invasion was initiated. Such glioma cell invasion was preserved even in the absence of FBS (Sup. Figure 1).

Glioma Cell Invasion is Cell Culture Specific

Seven different primary established GBM cultures were grafted as single tumorspheres in collagen matrix. For each culture 20 to 70 unique tumorsphere graftings, derived from at least three different passages, were performed. The invasive pattern displayed extensive intertumoral variations between cultures, but was stable for the individual culture (Sup. Figure 2). Although most experiments were done at early passages (<5), the invasive pattern was maintained even after long-time maintenance in vitro (up to passage 20).

We quantified the level of the invasion in five of the cultures using the estimation of the total number of invasive cells and the invasive increment sum to confirm the difference of invasion. The cultures could thus be ranked according to invasiveness (Figure 2, *A* and *B*). In five of the seven cultures we found that the invasive increment changed at a culture-specific distance from the tumor core, and this distance was reached within 48 hours. While invasive increment was stable close to the tumor core, cells lost directional movement and started to move randomly after reaching this limit ($P < .01$ in all analyzed samples). Beyond this, cells moved similar to what we observed in cell suspension grafts and after core resections. Such cells kept forming processes in alternating directions without resulting in directional advancement (Figure 2, *C–E*, Mov. 4). In the two cultures with the highest invasion (T1402 and T1456) invasive cells continued to migrate radially, accompanied by a gradual decrease of the tumor core density and size, and cells kept on migrating until they reached the border of the collagen gel.

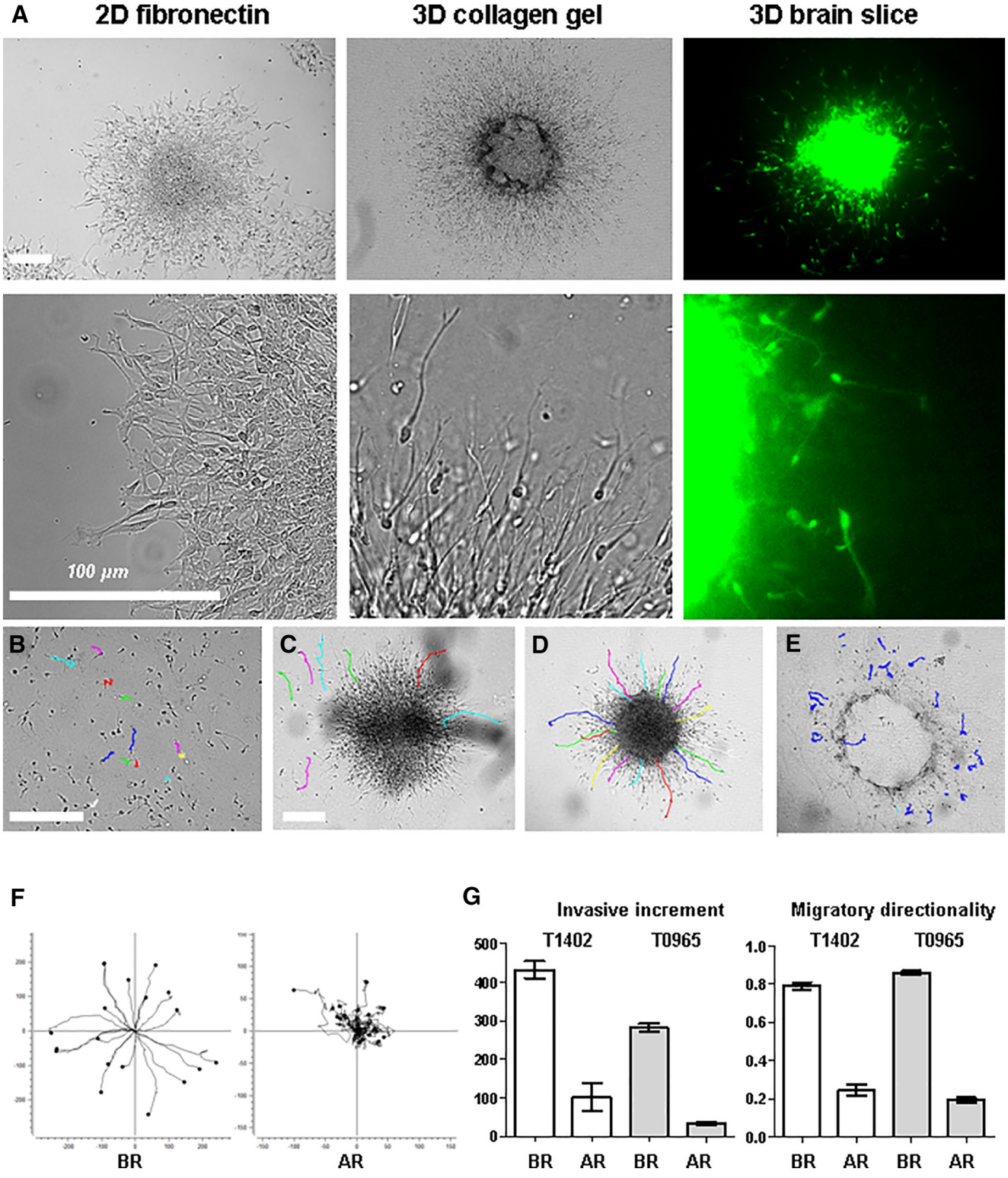

Figure 1. GBM cellular invasion is maintained in a simplified 3D-milieue by the presence of the core. A) Comparison between migration/invasion on 2D-fibronectin coating, 3D-collagen gel and rodent brain slices. The migration pattern of GBM cells in collagen gel grafted as suspension (B), suspension followed by co-grafting of tumorsphere (C), from tumorsphere (D) followed by the resection of the graft core (E). F) Representative GBM cell migration plots before and after graft core resection. BR – before core resection, AR – after core resection. G) Comparison of migratory directionality and invasive increment in T0965 and T1402 before and after core resection (46 to 87 tracked cells per observation).

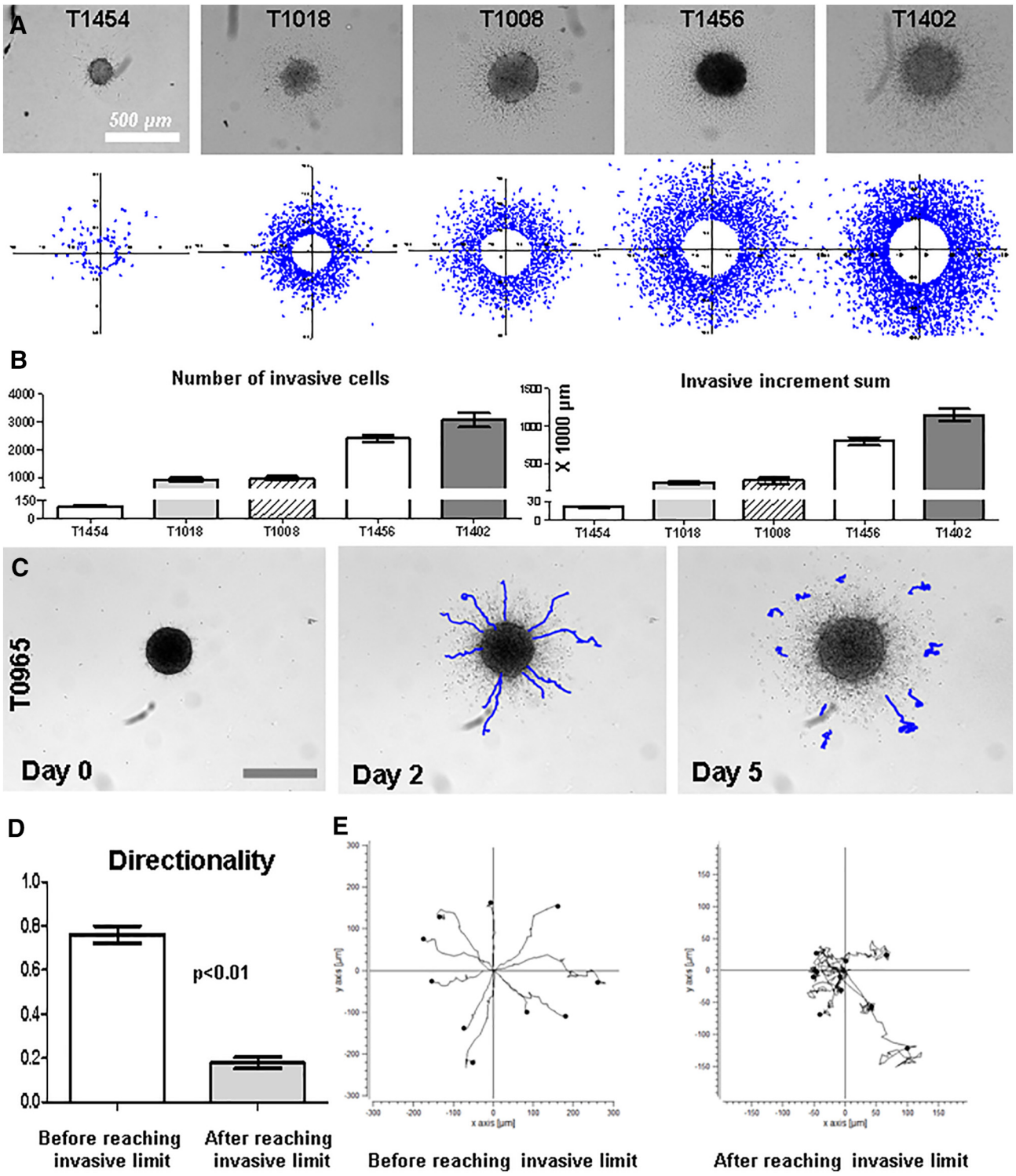

Figure 2. Glioma cell invasion is cell culture specific. A) Comparison between grafts from 5 different GBM cultures with plots representing the distribution of invasive cells after image-processing. B) Graphical representation of invasive characteristics. C) Time-lapse frames with cell tracks made immediately after grafting (Day 0), by Day 2 and 5 after grafting. D) Comparison of migrative directionality before and after reaching the "invasive limit" (38 tracked cells). E) Representative GBM cell migration plots before and after reaching the "invasive limit".

The Phenotype of Core and Invasive Cells

In the highly invasive T1402 and T1456 cultures the absolute majority of cells were Type I cells. The less invasive cultures had a much higher diversity of cellular phenotypes (Figure 3*A*), similar to our data obtained from GBM invasion in brain slices [12]. Interestingly, in the cell culture derived from a giant cell glioblastoma (T1559), the invasive population was dominated by giant cells. Similar giant cells were also found in other cultures, although rarely (Sup. Figure 2).

To further evaluate the phenotype of the invading glioma cells we performed staining for markers of neural stem cells, astrocytes and

neurons (nestin, GFAP and β-III-tubulin/MAP2, respectively). Despite differences in invasion patterns, all grafts were positive for all four markers (Sup. Figure 3, Mov. 5). All tumors had a similar pattern in marker distribution, with the overwhelming majority of cells being positive for nestin, β-III-tubulin and MAP2 both in the invasive front and in the tumor core. In contrast, GFAP staining was strongest in the core, and only a small proportion of the invasive cells were GFAP positive. qPCR-expression analysis verified the variation of GFAP found on immunochemistry (Sup. Figure 4).

To identify the movement pattern of specific cell populations, we used time-lapse imaging of cell cultures before fixation and immunostaining. $GFAP^+$ cells could then be backtracked on the time-lapse images to identify movement patterns. Analysis identified that the $GFAP^+$ cells had lower velocity than $nestin^+/GFAP^-$ cells and achieved smaller invasive increment: average velocity 0.12 ± 0.01 vs. 0.39 ± 0.4 μm/min, average invasive increment 86 ± 21 vs. 188 ± 47 μm in $GFAP^+$ vs. $nestin^+/GFAP^-$ invasive cells, respectively (Figure 3, *B–D*, Mov. 6). qPCR-expression analysis verified the variation of GFAP found on immunohistochemistry. The cultures with the highest invasive increment sum had the lowest expression of GFAP (Figure 3, *F–G*). In contrast, neither immunostaining nor qPCR could detect correlation between the level of β-III-tubulin expression and migratory capacity although this protein was present in the majority of the invasive cells in all cultures.

We observed cellular divisions and expression of Ki-67 in the invasive front (Sup. Figure 5). Interestingly, invasive cells were often positive for both Ki-67 and MAP2. Both markers were present in invasive cells that entered mitosis. We also used time-lapse recordings of invasion followed by imaging of markers on live or fixed samples (Sup. Figure 6). We could not identify any pattern in the staining distribution of the putative cancer stem/progenitor cell markers CXCR4, CD133, CD166, CD44, CD29 and CD9 related to the invasive properties of the cell cultures.

Grafted Core and Invasive Cells Have Significantly Different Gene Expression Profiles

To identify signaling cues that contribute to the directional cell movement, we analyzed gene expression in the core and the invasive front from three of the tumors grafted. We first investigated core and invasive cells in six grafts from the most invasive GBM culture (T1402), which allowed for a high number of invasive cells to be collected. Unsupervised hierarchical clustering of the samples separated core and invasive cells in two clusters. Rank analysis identified that 391 genes were significantly up- and down-regulated in invasive vs. core cells ($P < .01$, fold change >1.5). To identify signaling networks across cultures, we additionally included grafts from T1456 and T1008. The global gene expression differences between the cell cultures were larger than the gene expression differences found between invasive and core cells, as the individual cultures clustered separately (Figure 4*A*). The results from these microarrays were validated by qPCR of the 10 most dysregulated genes, and a high expression of annexin and CTGF in invasive cells was verified by immunofluorescence (Figures 4, *B–C*, 5*E*).

Cultures showed an overall difference in subtype profile using unsupervised hierarchical clustering according to Philips et al. [27]. The highly invasive T1402 culture showed enrichment of genes representing the mesenchymal subtype (CHI3L1, PDPN, FAM20C, SERPINE1) (Figure 4*D*). The less invasive cultures were more proneural-like (DLL3, NDRG2, SOX8), where the least invasive culture T1008 was more enriched in proneural genes than the more invasive culture T1456. Lineage markers were differently expressed between the cultures (Figure 4*E*). While all cultures expressed high levels of the progenitor markers NES, FABP7 and SOX2, markers of more differentiated neural lineages (GFAP, CSPG4 and MAP2) had highest expression in T1008. Markers of mesenchymal lineage (CHI3L1, PDPN, FAM2OC, SERPINE and CD44) had highest expression in the most invasive culture T1402.

Core Cells Display an Expression Signature of Genes Related to Response from Hypoxia and Include Chemo-Repulsive Signals

As invasive increment was dependent on the presence of a tumorsphere, we further identified a signature of highly expressed genes in the tumor core cells. These genes could be part of a signal to inhibit migration in core cells or a secreted signal to promote the chemo-repulsive effects on the invasive cells. To discern among these possibilities, the two cell cultures that clearly maintained a tumor core were used to establish the signature. Using the Rank product algorithm we identified a highly significant core signature of 73 genes (Q = 0), clearly separating the core and invasive cells (Figure 5 and Sup. Table 1). This signature could also separate core cells from invasive cells in the highly invasive T1402 culture. Interestingly, T1402 showed a stronger expression of this signature than T1456 and T1008, demonstrating that the signature was more related to chemo-repulsion than inhibition of migration. The signature included several genes known to be involved in response from hypoxia (VEGFA [28–30], ALDOC [31], ZNF395 [32], NDRG1 [33], DDIT4 [34]), as well as secreted signaling molecules suggested to play a role in invasion (VEGFA [35–37], AGT [38], NMB [39], ANGPTL4 [40], TF [41,42]).

Cells in the Invasive Front are Enriched in Genes Involved in Cell Survival and Aggressive Cancer

Similarly to the chemo-repulsive signature of core cells, we identified a signature of highly expressed genes in invasive cells in T1456 and T1008 by the Rank product algorithm. A significant invasive signature of 99 genes was identified (Q = 0), separating the core and invasive cells in (Figure 5 and Sup. Table 2). Unsupervised hierarchical clustering of these signature genes separated core and invasive cells in T1402, and their expression level in tumorsphere cultures under culturing conditions corresponded with the level of invasion identified in time-lapse experiments (T1402 > T1456 > T1008 > T0965). The invasive signature included genes known to be involved in regulation of cell cycle, cell survival and aggressive cancer such as MELK [43,44], BIRC5 [45], PBK [22], DLGAP5 [46] and CENPA [47]. The TWEAK receptor (TNFRSF12A) and CTGF were among the most dysregulated genes in the signature. We found CTGF to be highly expressed in invasive cells of T1402 on both western blot and immunocytochemistry. TNFRSF12A expression was confirmed on immunochemistry.

Discussion

We have previously used live brain slice cultures to explore invasion by cells expressing fluorescent probes [6]. In this study, we used a collagen matrix, which in contrast to the heterogeneous landscape of the brain-slice cultures allows for evaluation of single-cell movements at higher resolution and tracking of cells without the use of

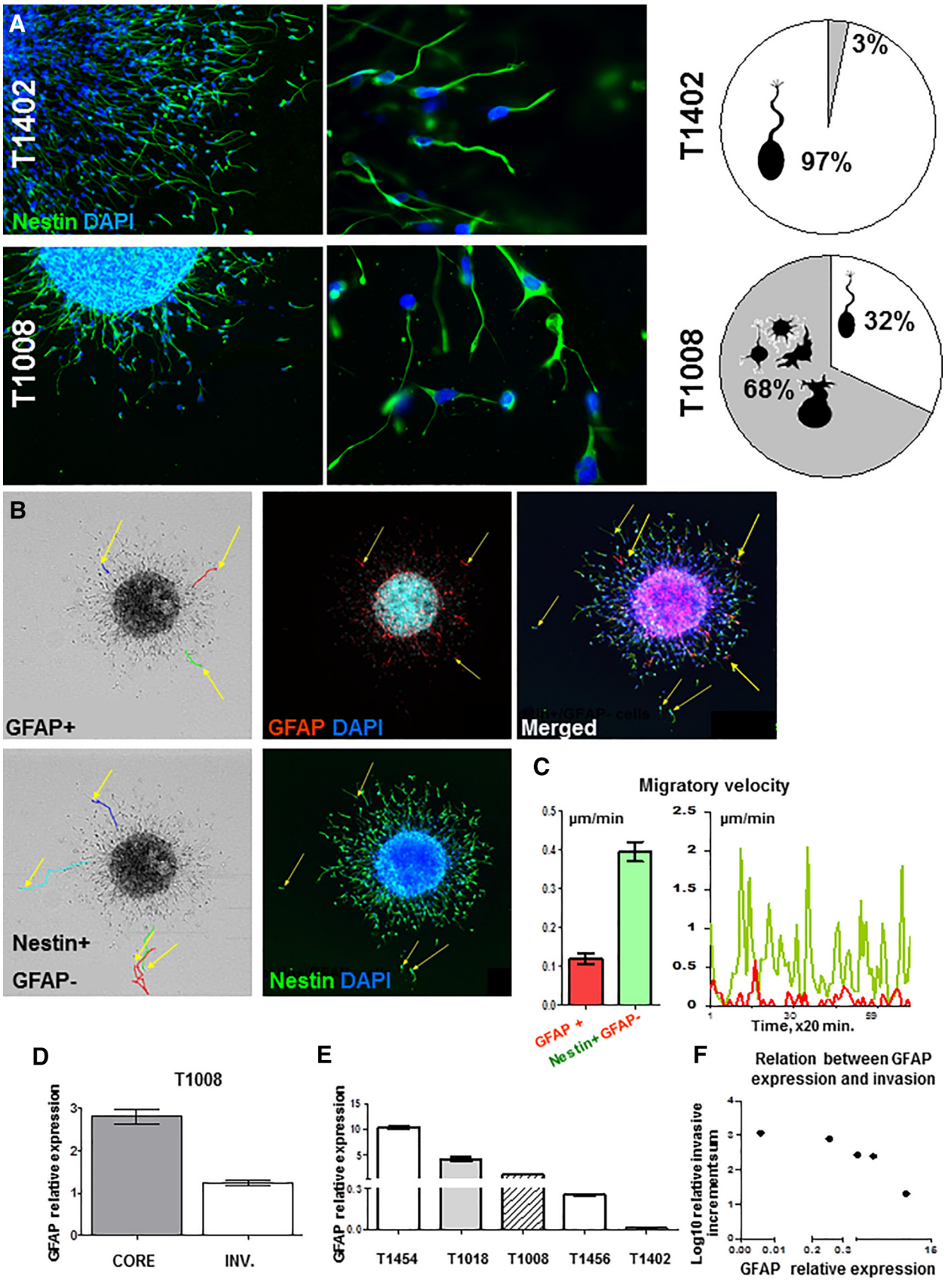

Figure 3. The phenotype of invasive cells. A) Comparison of invasive cell phenotype in moderately (T1008) and highly (T1402) invasive GBM grafts with sector diagrams representing the phenotypic composition of the invasive cell pool (100 cells per observation). B) Single cell tracking of GFAP$^+$ (n = 9) and nestin$^+$/GFAP$^-$ (n = 11) invasive cells and post-time-lapse immunostaining for GFAP, nestin and DAPI C) Migratory velocity of GFAP$^+$ and nestin$^+$/GFAP$^-$ invasive cells. D) GFAP expression in core and invasive cells (T1008). E) GFAP expression in invasive cells in five GBM cultures. F) Relation between GFAP expression in invasive cells and total invasive increment.

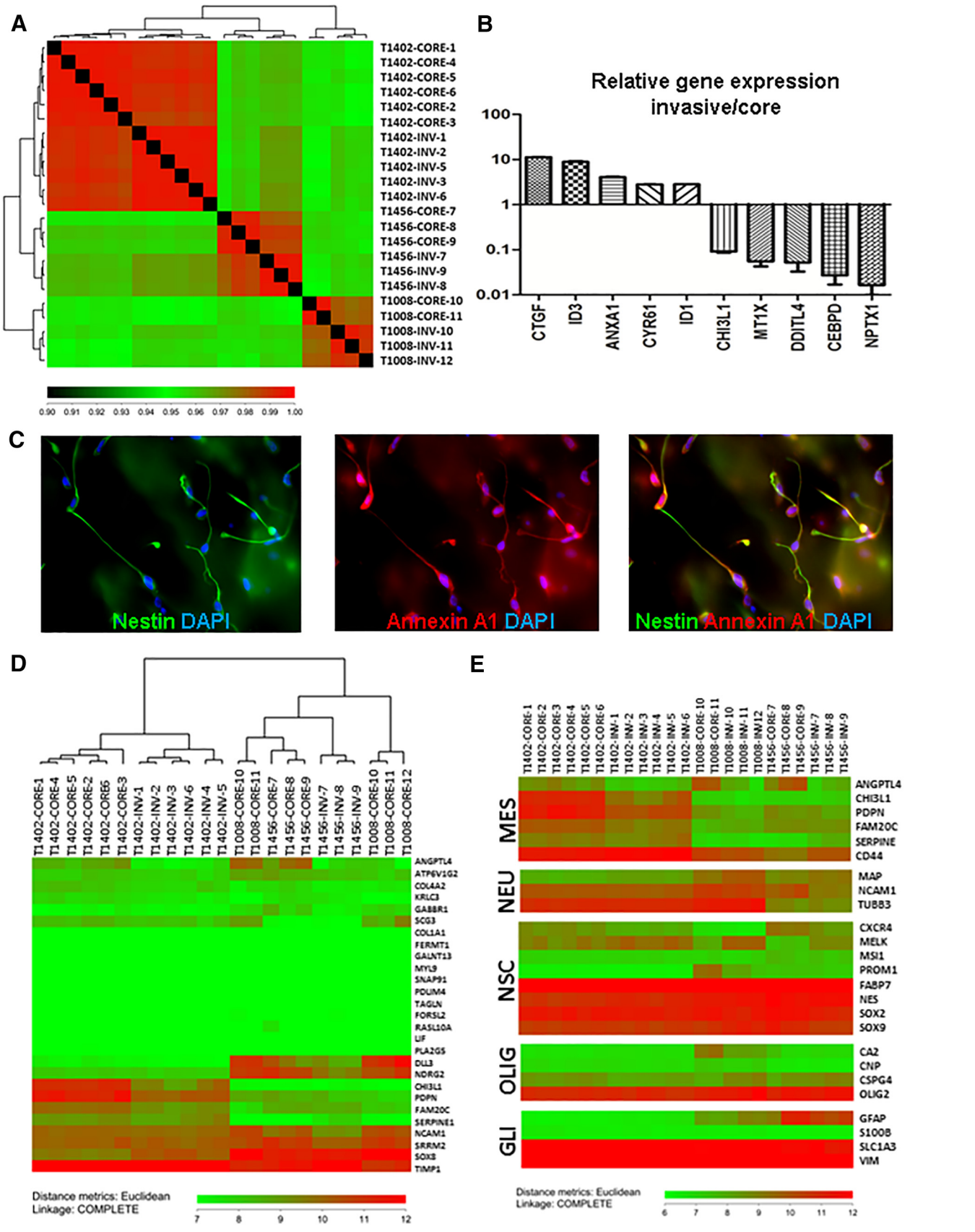

Figure 4. Grafted core and invasive cells have significantly different gene expression profiles. A) Unsupervised hierarchical clustering of microarray gene expression in core and invasive cells. B) Comparative qPCR relative expression of selected genes in invasive vs. core cells. C) Confirmation of annexin A1 expression in invasive cells by immunostaining. D) Unsupervised hierarchical clustering of microarray gene expression of genes according to Philips et al. [27]. E) Gene expression of lineage specific markers in core and invasive cells, astrocytes (GLI), oligodendrocytes (OLIG), neural stem cells (NSC), neurons (NEU) and mesenchymal cells (MES).

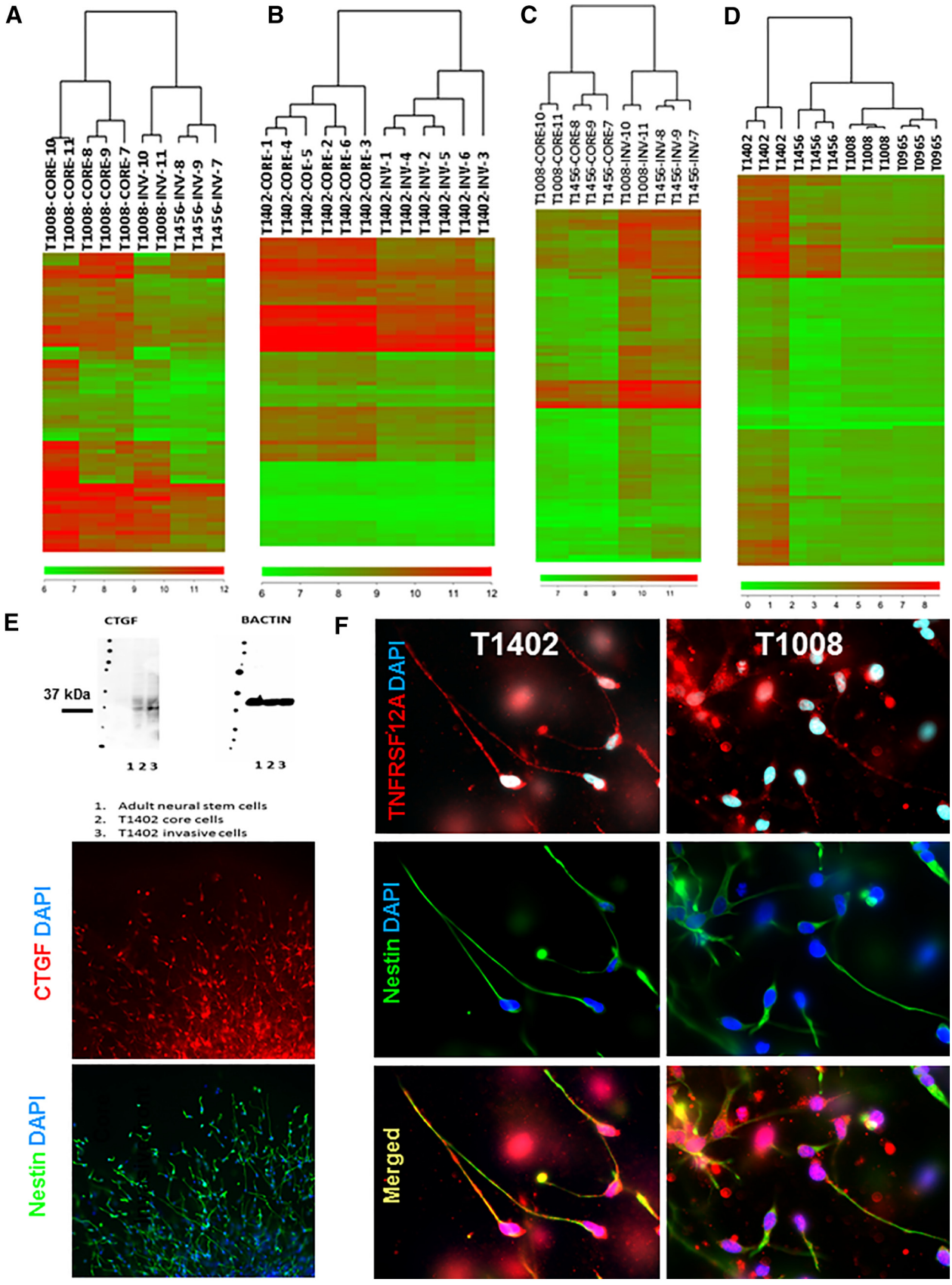

Figure 5. Core cells express genes related to hypoxia and chemo-repulsive signals, while cells in the invasive front express genes involved in cell survival and malignancy. A) A gene signature of core cells is identified in T1008 and T1456. B) The signature is also present in the highly invasive T1402. Since this culture disperses cells until no core is left, making all cells invasive, this signature characterizes a repulsive signal rather than a marker of stationary cells. C) A gene signature of invasive cells is identified in T1008 and T1456. D) The signature shows relationship between signature and invasiveness in four tumor cell cultures. E) Confirmation of CTGF expression in invasive cells by Western blot and immunostaining. F) Confirmation of TNRS12AF expression in invasive cells by immunostaining.

fluorescent labeling. The stability of the invasive cellular phenotype between different GBM cultures and the presence of a cell culture specific magnitude of invasion suggests that this model recapitulates the variance in tumor cell dispersal seen in patients.

The assay is clearly a great simplification, even compared to the brain-slice invasion assay. [48]. Vascular cells, microglia, peripheral immune cells, neural progenitors, and mature neural cells all contribute to the disease evolution [49]. In the present work we strived to limit the number of variables, leaving only the core, invasive cells and 3D matrix as the scaffold for invasion.

The Signaling From the Core of Grafted GBM Tumorspheres Plays a Crucial Role in Promoting Invasion

Several studies have shown that selected proteins guide both neural and glial precursors in the developing brain and play a crucial role in axon guidance: netrins, semaphorins, slit-family proteins, PDGF, HGF and others [50]. Neural stem cells and glioma cells may follow similar topical cues. Glioma tumorspheres release factors that direct cells away from the implanted spheroid in 3D-matrixes by repellent signals [50–52]. The magnitude of invasion has been correlated with the hypoxia level in the necrotic center of the implanted spheres [52]. The stressful conditions in the hypoxic core, such as decreased pH, a low level of oxygen and accumulation of metabolic substrates may lead to the generation of repellent factors and a concentration gradient. This results in driving cell invasion from the core and invasion arrest when the gradient is no longer present [50]. Our gene expression signature from tumor core cells support that such signaling is related to long distance migration. By functional time-lapse experiments, we also show that signaling from the tumorsphere is dictating the range and direction of GBM cell invasion. While cellular directionality and speed are affected over distance, enablement of cells to initiate invasion away from the sphere could be regulated though other mechanisms, as, for example, contact inhibition. It has been shown that contact inhibition is involved in switching from restrained to invasive migration of cancer cells [53].

The gene expression data suggests that the repulsive signal produced by the tumorsphere is highest in tumors of the mesenchymal subtype. This does not fit well with a published study on the analysis of tumor samples obtained during surgery, where biopsies from the tumor core showed the highest correlation with the mesenchymal and classical subtypes, whilst biopsies from the invasive area have the highest correlation with the proneural subtypes [16]. This discrepancy might be due technical considerations, as the biopsies from the invasive area would definitely contain normal brain tissue tilting the expression towards a proneural subtype.

The signature of tumor cores encompasses signaling related to hypoxia and neovascularization, where VEGFA was among the most highly regulated genes. Besides playing a crucial role in physiological angiogenesis and tumor neovascularization, VEGF binds to neuropilin/plexin receptors – the primary receptors for the semaphorin family of proteins. These proteins are central to the control of directed migration of neural progenitor cells [54]. Since VEGF and semaphorins can bind to the same receptor, the VEGF-signaling cascade could be important in orchestrating the chemorepulsive signals in driving GBM migration [55].

The Invasive Glioma Cell Phenotype

Migrating glioma cells display a phenotype similar to migrating neural progenitors. This could be an adaptation to migration through the complex extracellular environment of the brain [56,57]. This phenotype, which we call Type I, can be found at the invasive front in both the complex neuropil of brain slice cultures and in the simple 3D collagen matrix suggests that this phenotype is cell-type intrinsic and not a secondary to the extracellular milieu. The fact that other types of non-glial cancer cells move through collagen 3D matrixes by lamellipodia-based or amoeboid migration [58], without displaying this Type I phenotype, supports this interpretation.

The migratory Type I cells with the highest invasion were GFAP negative. Interestingly, others have shown that GFAP overexpression inhibits glioma cell motility [55] and that down-regulation of GFAP expression is often seen in high-grade gliomas in vivo [59]. Also, cultures with higher invasive increment had lower levels of neural lineage markers, and expressed genes associated with a mesenchymal subtype or lineage. This fits well with a transition towards a mesenchymal expression upon tumor progression [27]. Furthermore, our data highlights the malignancy of the highly invasive cells. Not only do they have the ability to escape tumor resection, but they maintain the ability to proliferate as demonstrated by time-lapse records, Ki-67 staining and overexpressing genes related to the cell cycle and resistance to cell death.

The invasive cells overexpress a number of genes, among which TNFRSF12A and CTGF were most notable. The expression of TNFRSF12A receptor gene is up-regulated in migrating glioma cells in vitro and overexpressed in the invasive rim of cells in surgical glioma specimens [60] and, in particular, in GBMs exhibiting the mesenchymal molecular subtype [61]. As its overexpression is associated with invasion and resistance to chemotherapeutic agents in vitro, TNFRSF12A is suggested as a potential cell surface portal for targeted delivery of anti-GBM therapeutics [61]. CYR61 and CTGF have also previously been shown to be important for glioma motility in vitro [15] and are associated with prognosis, survival and drug resistance in patients with gliomas [62,63].

Clinical experience demonstrates that invasion is present in all glioblastoma tumors, but to a varying degree. This is consistent with the in vitro data we present here. The overwhelming majority of current strategies to influence the cancer invasion aims to inhibit the tumor cells ability to migrate [64]. In GBM this has little sense: at the moment of diagnosis the GBM cells has already spread through the brain due to the extremely high invasive properties. Blocking or reducing the migratory ability of the GBM cells – that are already at the distant site from the main bulk – would have little effects on tumor spread. Thus, new strategies should selectively target the cells that already invaded in to the brain, eliminate their tumorigenic potential, or force them to change their migratory path in order to make them become more "available" for targeted therapy, such as surgery or focused irradiation [65]. We hope the presented data would add to this understanding.

Conclusion

Although being performed in a simple system, time-lapse imaging of GBM cells in a collagen matrix displays intertumoral variations of invasion pattern. The pro-invasive signaling differs in strength between patient derived cultures, similar to what we see in the clinical setting. We show that glioblastoma tumorsphere core promotes invasion of a defined subpopulation of tumor cells.

Transcriptional differences between invasive and core cells suggest that invasive cells may be manipulated to affect brain tumor behavior with a consequence on treatment outcome. Both the phenotypically

specified invasive cells and the identified pro-migratory signals bear potential for therapy development.

Supplementary data to this article can be found online at https://doi.org/10.1016/j.tranon.2018.09.014.

Acknowledgements

This study was funded through the Norwegian Cancer Society (#2326811, #144402). We thank Sissel Reinlie, the Head of Neurosurgical Department, Oslo University Hospital and Håvard Attramadal, the Head of Institute for Surgical Research for support and excellent working environment, Emily Telmo and Jinan Behnan for primary processing of tumor tissues and cell culturing.

References

[1] Ronning PA, Helseth E, Meling TR, and Johannesen TB (2012). A population-based study on the effect of temozolomide in the treatment of glioblastoma multiforme. *Neuro Oncol* **14**(9), 1178–1184.

[2] Chen J, Li Y, Yu TS, McKay RM, Burns DK, Kernie SG, and Parada LF (2012). A restricted cell population propagates glioblastoma growth after chemotherapy. *Nature* **488**(7412), 522–526.

[3] Amberger-Murphy V (2009). Hypoxia helps glioma to fight therapy. *Curr Cancer Drug Targets* **9**(3), 381–390.

[4] Beauchesne P (2011). Extra-neural metastases of malignant gliomas: Myth or reality? *Cancers (Basel)* **3**(1), 461–477.

[5] Cuddapah VA, Robel S, Watkins S, and Sontheimer H (2014). A neurocentric perspective on glioma invasion. *Nat Rev Neurosci* **15**(7), 455–465.

[6] Li A, Walling J, Ahn S, Kotliarov Y, Su Q, Quezado M, Oberholtzer JC, Park J, Zenklusen JC, and Fine HA (2009). Unsupervised analysis of transcriptomic profiles reveals six glioma subtypes. *Cancer Res* **69**(5), 2091–2099.

[7] Lee J, Kotliarova S, Kotliarov Y, Li A, Su Q, Donin NM, Pastorino S, Purow BW, Christopher N, and Zhang W, et al (2006). Tumor stem cells derived from glioblastomas cultured in bfgf and egf more closely mirror the phenotype and genotype of primary tumors than do serum-cultured cell lines. *Cancer Cell* **9**(5), 391–403.

[8] Huszthy PC, Daphu I, Niclou SP, Stieber D, Nigro JM, Sakariassen PO, Miletic H, Thorsen F, and Bjerkvig R (2012). In vivo models of primary brain tumors: Pitfalls and perspectives. *Neuro Oncol* **14**(8), 979–993.

[9] Galli R, Binda E, Orfanelli U, Cipelletti B, Gritti A, De Vitis S, Fiocco R, Foroni C, Dimeco F, and Vescovi A (2004). Isolation and characterization of tumorigenic, stem-like neural precursors from human glioblastoma. *Cancer Res* **64**(19), 7011–7021.

[10] Singh SK, Clarke ID, Hide T, and Dirks PB (2004). Cancer stem cells in nervous system tumors. *Oncogene* **23**(43), 7267–7273.

[11] Varghese M, Olstorn H, Sandberg C, Vik-Mo EO, Noordhuis P, Nister M, Berg-Johnsen J, Moe MC, and Langmoen IA (2008). A comparison between stem cells from the adult human brain and from brain tumors. *Neurosurgery* **63**(6), 1022–1033 [discussion 1033-1024].

[12] Fayzullin A, Tuvnes FA, Skjellegrind HK, Behnan J, Mughal AA, Langmoen IA, and Vik-Mo EO (2016). Time-lapse phenotyping of invasive glioma cells ex vivo reveals subtype-specific movement patterns guided by tumor core signaling. *Exp Cell Res* **349**(2), 199–213.

[13] Keunen O, Johansson M, Oudin A, Sanzey M, Rahim SA, Fack F, Thorsen F, Taxt T, Bartos M, and Jirik R, et al (2011). Anti-vegf treatment reduces blood supply and increases tumor cell invasion in glioblastoma. *Proc Natl Acad Sci U S A* **108**(9), 3749–3754.

[14] Hoelzinger DB, Mariani L, Weis J, Woyke T, Berens TJ, McDonough WS, Sloan A, Coons SW, and Berens ME (2005). Gene expression profile of glioblastoma multiforme invasive phenotype points to new therapeutic targets. *Neoplasia* **7**(1), 7–16.

[15] Demuth T, Rennert JL, Hoelzinger DB, Reavie LB, Nakada M, Beaudry C, Nakada S, Anderson EM, Henrichs AN, and McDonough WS, et al (2008). Glioma cells on the run - the migratory transcriptome of 10 human glioma cell lines. *BMC Genomics* **9**, 54.

[16] Aubry M, de Tayrac M, Etcheverry A, Clavreul A, Saikali S, Menei P, and Mosser J (2015). From the core to beyond the margin: A genomic picture of glioblastoma intratumor heterogeneity. *Oncotarget* **6**(14), 12094–12109.

[17] Holtkamp N, Afanasieva A, Elstner A, van Landeghem FK, Konneker M, Kuhn SA, Kettenmann H, and von Deimling A (2005). Brain slice invasion model reveals genes differentially regulated in glioma invasion. *Biochem Biophys Res Commun* **336**(4), 1227–1233.

[18] Nevo I, Woolard K, Cam M, Li A, Webster JD, Kotliarov Y, Kim HS, Ahn S, Walling J, and Kotliarova S, et al (2014). Identification of molecular pathways facilitating glioma cell invasion in situ. *PLoS One* **9**(11)e111783.

[19] Parker JJ, Dionne KR, Massarwa R, Klaassen M, Foreman NK, Niswander L, Canoll P, Kleinschmidt-Demasters BK, and Waziri A (2013). Gefitinib selectively inhibits tumor cell migration in egfr-amplified human glioblastoma. *Neuro Oncol* **15**(8), 1048–1057.

[20] Vik-Mo EO, Sandberg C, Olstorn H, Varghese M, Brandal P, Ramm-Pettersen J, Murrell W, and Langmoen IA (2010). Brain tumor stem cells maintain overall phenotype and tumorigenicity after in vitro culturing in serum-free conditions. *Neuro Oncol* **12**(12), 1220–1230.

[21] Mughal AA, Grieg Z, Skjellegrind H, Fayzullin A, Lamkhannat M, Joel M, Ahmed MS, Murrell W, Vik-Mo EO, and Langmoen IA, et al (2015). Knockdown of nat12/naa30 reduces tumorigenic features of glioblastoma-initiating cells. *Mol Cancer* **14**, 160.

[22] Joel M, Mughal AA, Grieg Z, Murrell W, Palmero S, Mikkelsen B, Fjerdingstad HB, Sandberg CJ, Behnan J, and Glover JC, et al (2015). Targeting pbk/topk decreases growth and survival of glioma initiating cells in vitro and attenuates tumor growth in vivo. *Mol Cancer* **14**, 121.

[23] Skjellegrind HK, Fayzullin A, Johnsen EO, Eide L, Langmoen IA, Moe MC, and Vik-Mo EO (2016). Short-term differentiation of glioblastoma stem cells induces hypoxia tolerance. *Neurochem Res* **41**(7), 1545–1558.

[24] Kierulf-Vieira KS, Sandberg CJ, Grieg Z, Gunther CC, Langmoen IA, and Vik-Mo EO (2016). Wnt inhibition is dysregulated in gliomas and its re-establishment inhibits proliferation and tumor sphere formation. *Exp Cell Res* **340**(1), 53–61.

[25] Hong F, Breitling R, McEntee CW, Wittner BS, Nemhauser JL, and Chory J (2006). Rankprod: A bioconductor package for detecting differentially expressed genes in meta-analysis. *Bioinformatics* **22**(22), 2825–2827.

[26] Rao SS, Dejesus J, Short AR, Otero JJ, Sarkar A, and Winter JO (2013). Glioblastoma behaviors in three-dimensional collagen-hyaluronan composite hydrogels. *ACS Appl Mater Interfaces* **5**(19), 9276–9284.

[27] Phillips HS, Kharbanda S, Chen R, Forrest WF, Soriano RH, Wu TD, Misra A, Nigro JM, Colman H, and Soroceanu L, et al (2006). Molecular subclasses of high-grade glioma predict prognosis, delineate a pattern of disease progression, and resemble stages in neurogenesis. *Cancer Cell* **9**(3), 157–173.

[28] Ido K, Nakagawa T, Sakuma T, Takeuchi H, Sato K, and Kubota T (2008). Expression of vascular endothelial growth factor-a and mrna stability factor hur in human astrocytic tumors. *Neuropathology* **28**(6), 604–611.

[29] Shweiki D, Itin A, Soffer D, and Keshet E (1992). Vascular endothelial growth factor induced by hypoxia may mediate hypoxia-initiated angiogenesis. *Nature* **359**(6398), 843–845.

[30] Terashima J, Sampei S, Iidzuka M, Ohsakama A, Tachikawa C, Satoh J, Kudo K, Habano W, and Ozawa S (2016). Vegf expression is regulated by hif-1alpha and arnt in 3d kyse-70, esophageal cancer cell spheroids. *Cell Biol Int* **40**(11), 1187–1194.

[31] Kathagen-Buhmann A, Schulte A, Weller J, Holz M, Herold-Mende C, Glass R, and Lamszus K (2016). Glycolysis and the pentose phosphate pathway are differentially associated with the dichotomous regulation of glioblastoma cell migration versus proliferation. *Neuro Oncol* **18**(9), 1219–1229.

[32] Murat A, Migliavacca E, Hussain SF, Heimberger AB, Desbaillets I, Hamou MF, Ruegg C, Stupp R, Delorenzi M, and Hegi ME (2009). Modulation of angiogenic and inflammatory response in glioblastoma by hypoxia. *PLoS One* **4**(6)e5947.

[33] Said HM, Stein S, Hagemann C, Polat B, Staab A, Anacker J, Schoemig B, Theobald M, Flentje M, and Vordermark D (2009). Oxygen-dependent regulation of ndrg1 in human glioblastoma cells in vitro and in vivo. *Oncol Rep* **21**(1), 237–246.

[34] Lee CH, Park JH, Cho JH, Ahn JH, Yan BC, Lee JC, Shin MC, Cheon SH, Cho YS, and Cho JH, et al (2014). Changes and expressions of redd1 in neurons and glial cells in the gerbil hippocampus proper following transient global cerebral ischemia. *J Neurol Sci* **344**(1-2), 43–50.

[35] Zeng FC, Zeng MQ, Huang L, Li YL, Gao BM, Chen JJ, Xue RZ, and Tang ZY (2016). Downregulation of vegfa inhibits proliferation, promotes apoptosis, and suppresses migration and invasion of renal clear cell carcinoma. *Onco Targets Ther* **9**, 2131–2141.

[36] Zhang L, Wang JN, Tang JM, Kong X, Yang JY, Zheng F, Guo LY, Huang YZ, Zhang L, and Tian L, et al (2012). Vegf is essential for the growth and migration of human hepatocellular carcinoma cells. *Mol Biol Rep* **39**(5), 5085–5093.

[37] Oommen S, Gupta SK, and Vlahakis NE (2011). Vascular endothelial growth factor a (vegf-a) induces endothelial and cancer cell migration through direct binding to integrin {alpha}9{beta}1: Identification of a specific {alpha}9{beta}1 binding site. *J Biol Chem* **286**(2), 1083–1092.

[38] Rodrigues-Ferreira S, Abdelkarim M, Dillenburg-Pilla P, Luissint AC, di-Tommaso A, Deshayes F, Pontes CL, Molina A, Cagnard N, and Letourneur F, et al (2012). Angiotensin ii facilitates breast cancer cell migration and metastasis. *PLoS One* **7**(4), e35667.

[39] Park HJ, Kim MK, Choi KS, Jeong JW, Bae SK, Kim HJ, and Bae MK (2016). Neuromedin b receptor antagonism inhibits migration, invasion, and epithelial-mesenchymal transition of breast cancer cells. *Int J Oncol* **49**(3), 934–942.

[40] Katanasaka Y, Kodera Y, Kitamura Y, Morimoto T, Tamura T, and Koizumi F (2013). Epidermal growth factor receptor variant type iii markedly accelerates angiogenesis and tumor growth via inducing c-myc mediated angiopoietin-like 4 expression in malignant glioma. *Mol Cancer* **12**, 31.

[41] Gessler F, Voss V, Dutzmann S, Seifert V, Gerlach R, and Kogel D (2010). Inhibition of tissue factor/protease-activated receptor-2 signaling limits proliferation, migration and invasion of malignant glioma cells. *Neuroscience* **165**(4), 1312–1322.

[42] Harter PN, Dutzmann S, Drott U, Zachskorn C, Hattingen E, Capper D, Gessler F, Senft C, Seifert V, and Plate KH, et al (2013). Anti-tissue factor (tf9-10h10) treatment reduces tumor cell invasiveness in a novel migratory glioma model. *Neuropathology* **33**(5), 515–525.

[43] Simon M, Mesmar F, Helguero L, and Williams C (2017). Genome-wide effects of melk-inhibitor in triple-negative breast cancer cells indicate context-dependent response with p53 as a key determinant. *PLoS One* **12**(2)e0172832.

[44] Speers C, Zhao SG, Kothari V, Santola A, Liu M, Wilder-Romans K, Evans J, Batra N, Bartelink H, and Hayes DF, et al (2016). Maternal embryonic leucine zipper kinase (melk) as a novel mediator and biomarker of radioresistance in human breast cancer. *Clin Cancer Res* **22**(23), 5864–5875.

[45] Shamsabadi FT, Eidgahi MR, Mehrbod P, Daneshvar N, Allaudin ZN, Yamchi A, and Shahbazi M (2016). Survivin, a promising gene for targeted cancer treatment. *Asian Pac J Cancer Prev* **17**(8), 3711–3719.

[46] Schneider MA, Christopoulos P, Muley T, Warth A, Klingmueller U, Thomas M, Herth FJ, Dienemann H, Mueller NS, and Theis F, et al (2017). Aurka, dlgap5, tpx2, kif11 and ckap5: Five specific mitosis-associated genes correlate with poor prognosis for non-small cell lung cancer patients. *Int J Oncol* **50**(2), 365–372.

[47] Stangeland B, Mughal AA, Grieg Z, Sandberg CJ, Joel M, Nygard S, Meling T, Murrell W, Vik Mo EO, and Langmoen IA (2015). Combined expressional analysis, bioinformatics and targeted proteomics identify new potential therapeutic targets in glioblastoma stem cells. *Oncotarget* **6**(28), 26192–26215.

[48] Xiao W, Sohrabi A, and Seidlits SK (2017). Integrating the glioblastoma microenvironment into engineered experimental models. *Future Sci OA* **3**(3)Fso189.

[49] Charles NA, Holland EC, Gilbertson R, Glass R, and Kettenmann H (2012). The brain tumor microenvironment. *Glia* **60**(3), 502–514.

[50] Werbowetski T, Bjerkvig R, and Del Maestro RF (2004). Evidence for a secreted chemorepellent that directs glioma cell invasion. *J Neurobiol* **60**(1), 71–88.

[51] Maestro RD, Shivers R, McDonald W, and Maestro AD (2001). Dynamics of c6 astrocytoma invasion into three-dimensional collagen gels. *J Neuro-Oncol* **53**(2), 87–98.

[52] Tamaki M, McDonald W, Amberger VR, Moore E, and Del Maestro RF (1997). Implantation of c6 astrocytoma spheroid into collagen type i gels: Invasive, proliferative, and enzymatic characterizations. *J Neurosurg* **87**(4), 602–609.

[53] Astin JW, Batson J, Kadir S, Charlet J, Persad RA, Gillatt D, Oxley JD, and Nobes CD (2010). Competition amongst eph receptors regulates contact inhibition of locomotion and invasiveness in prostate cancer cells. *Nat Cell Biol* **12**(12), 1194–1204.

[54] Hu B, Guo P, Bar-Joseph I, Imanishi Y, Jarzynka MJ, Bogler O, Mikkelsen T, Hirose T, Nishikawa R, and Cheng SY (2007). Neuropilin-1 promotes human glioma progression through potentiating the activity of the hgf/sf autocrine pathway. *Oncogene* **26**(38), 5577–5586.

[55] Farin A, Suzuki SO, Weiker M, Goldman JE, Bruce JN, and Canoll P (2006). Transplanted glioma cells migrate and proliferate on host brain vasculature: A dynamic analysis. *Glia* **53**(8), 799–808.

[56] Beadle C, Assanah MC, Monzo P, Vallee R, Rosenfeld SS, and Canoll P (2008). The role of myosin ii in glioma invasion of the brain. *Mol Biol Cell* **19**(8), 3357–3368.

[57] Petrie RJ and Yamada KM (2012). At the leading edge of three-dimensional cell migration. *J Cell Sci* **125**(Pt 24), 5917–5926.

[58] Elobeid A, Bongcam-Rudloff E, Westermark B, and Nister M (2000). Effects of inducible glial fibrillary acidic protein on glioma cell motility and proliferation. *J Neurosci Res* **60**(2), 245–256.

[59] Wilhelmsson U, Eliasson C, Bjerkvig R, and Pekny M (2003). Loss of gfap expression in high-grade astrocytomas does not contribute to tumor development or progression. *Oncogene* **22**(22), 3407–3411.

[60] Tran NL, McDonough WS, Savitch BA, Fortin SP, Winkles JA, Symons M, Nakada M, Cunliffe HE, Hostetter G, and Hoelzinger DB, et al (2006). Increased fibroblast growth factor-inducible 14 expression levels promote glioma cell invasion via rac1 and nuclear factor-kappab and correlate with poor patient outcome. *Cancer Res* **66**(19), 9535–9542.

[61] Perez JG, Tran NL, Rosenblum MG, Schneider CS, Connolly NP, Kim AJ, Woodworth GF, and Winkles JA (2016). The tweak receptor fn14 is a potential cell surface portal for targeted delivery of glioblastoma therapeutics. *Oncogene* **35**(17), 2145–2155.

[62] Xie D, Yin D, Wang HJ, Liu GT, Elashoff R, Black K, and Koeffler HP (2004). Levels of expression of cyr61 and ctgf are prognostic for tumor progression and survival of individuals with gliomas. *Clin Cancer Res* **10**(6), 2072–2081.

[63] Yin D, Chen W, O'Kelly J, Lu D, Ham M, Doan NB, Xie D, Wang C, Vadgama J, and Said JW, et al (2010). Connective tissue growth factor associated with oncogenic activities and drug resistance in glioblastoma multiforme. *Int J Cancer* **127**(10), 2257–2267.

[64] Veiseh O, Kievit FM, Ellenbogen RG, and Zhang M (2011). Cancer cell invasion: Treatment and monitoring opportunities in nanomedicine. *Adv Drug Deliv Rev* **63**(8), 582–596.

[65] Jain A, Betancur M, Patel GD, Valmikinathan CM, Mukhatyar VJ, Vakharia A, Pai SB, Brahma B, MacDonald TJ, and Bellamkonda RV (2014). Guiding intracortical brain tumour cells to an extracortical cytotoxic hydrogel using aligned polymeric nanofibres. *Nat Mater* **13**(3), 308–316.